Impact of Slotframe Length on Performance of TSCH-Based Wireless Powered Sensor Networks

Sol-Bee Lee
Division of Software
Hallym University
Chuncheon, South Korea
thfqla3535@hallym.ac.kr

Jung-Hyok Kwon
Smart Computing Laboratory
Hallym University
Chuncheon, South Korea
jhkwon@hallym.ac.kr

Eui-Jik Kim*
Division of Software
Hallym University
Chuncheon, South Korea
ejkim32@hallym.ac.kr

2023 13th International Conference on Power, Energy and Electrical Engineering (CPEEE) | 978-1-6654-9014-6/23/$31.00 ©2023 IEEE | DOI: 10.1109/CPEEE56777.2023.10217696

***Abstract*—Recently, the IEEE 802.15.4 time-slotted channel hopping (TSCH) has been considered one of the emerging medium access control (MAC) protocols for the low-power and highly reliable wireless powered sensor networks (WPSNs). In TSCH-based WPSN, the period of data transmission and energy harvesting is determined depending on the slotframe length. Thus, the slotframe length may largely affect the performance of TSCH-based WPSN, especially when the network environment varies. Accordingly, in the TSCH-based WPSN design, it is considered an important issue to determine an appropriate slotframe length in consideration of the network environment. In this paper, we investigate the impact of slotframe length on the performance of TSCH-based WPSNs through experimental simulation. Specifically, we observe the variation of the total amount of harvested energy, aggregate throughput, and average end-to-end delay when the network size and traffic load change and discuss the appropriate slotframe length for different network environments.**

Keywords—energy harvesting, IEEE 802.15.4 TSCH, slotframe length, WPSN, WPT

I. INTRODUCTION

Over the decades, the wireless sensor network (WSN) has played a key role in the Internet of Things (IoT) system such as monitoring, tracking, management, and remote control [1–2]. In WSNs, a number of low-power and battery-powered sensor nodes require frequent recharging and replacement of battery due to the limited battery capacity [3]. Recently, radio frequency (RF)-based wireless power transfer (WPT) technology is emerging as a promising solution to the battery problem of sensor nodes [4–5]. The WPT enables sensor nodes to harvest energy from adjacent power transmitters. Thus, WSNs applied RF-based WPT—wireless powered sensor networks (WPSNs)—are considered one of the key driving forces to achieve sustainable operation for IoT.

The WPSN consists of hybrid access points (HAPs) serving as power transmitters and sensor nodes. In general, the HAP powered by the grid performs WPT and collects data from sensor nodes. The sensor node performs energy harvesting and transmits data to the HAP. According to the nature of WPSN where both WPT and data transmission between HAPs and sensor nodes, the WPSN forms a cluster-tree network topology in which HAPs act as cluster heads. Therefore, HAPs need to supply a sufficient amount of power to sensor nodes in a timely manner so that sensor nodes can operate stably without suffering from energy depletion. To this end, a medium access control (MAC) protocol should efficiently determine when and how long the HAPs transfer power, and when and how long the sensor nodes harvest energy while minimizing the energy consumption of sensor nodes in the network.

Time-slotted channel hopping (TSCH), the time-division multiple access (TDMA)-based MAC protocol specified in IEEE 802.15.4-2015 [6], is designed to provide low-power consumption of energy-constrained sensor nodes. It allows sensor nodes to reduce the energy consumption derived by contention and retransmission through the use of slotframe structure based on the combination of time-slotted access with multi-channel and channel hopping. The slotframe is a collection of cells expressed by timeslot and channel offset and is repeated over time. In addition, the sensor nodes can save energy by maintaining the sleep state when they have no allocated cell at a specific timeslot. In this respect, TSCH can be considered as a suitable MAC protocol for WPSNs. However, as the slotframe is periodically repeated, an inappropriate slotframe length (i.e., the number of timeslots) can result in degradation in the amount of energy harvested by the sensor node and network performance. Thus, the slotframe length is regarded as a key concern to achieve energy-efficient TSCH-based WPSN.

In this paper, we investigated the impact of slotframe length on the performance of TSCH-based WPSNs to determine an appropriate slotframe length considering the network environment. For this, the experimental simulation was conducted using the MATLAB simulator. Then, the performance in terms of the total amount of harvested energy, aggregate throughput, and average end-to-end delay was observed. From the results, we obtained that the slotframe length that maximizes the total amount of harvested energy and aggregate throughput highly relies on the number of sensor nodes and traffic load. We also derived that the longer the slotframe length, the longer the average end-to-end delay.

The remainder of this paper is organized as follows. Section II describes an overview of TSCH. Section III presents a system model for TSCH-based WPSN. We provide the simulation configuration and results in Section IV. Finally, Section V concludes this paper.

*Corresponding Author: ejkim32@hallym.ac.kr

II. BACKGROUND

This section provides an overview of TSCH. TSCH is a MAC protocol for low-power and lossy networks standardized in the IEEE 802.15.4-2015 [6], which provides highly reliable communications and deterministic delay between nodes based on time-slotted access with multi-channel and channel hopping mechanism. TSCH uses a slotframe structure composed of multiple cells as shown in Fig. 1. A cell is identified by a pair of timeslot and channel offset within the slotframe and is long enough to exchange a single frame and an acknowledgment (Ack). It is typically 10 ms long and can be scheduled as a dedicated cell or a shared cell. In the dedicated cell, only a pair of nodes can transmit a frame without contention. In contrast, multiple nodes can access the same channel at the same time in the shared cell.

For channel hopping, the channel of each cell is determined as follows:

$$Channel = f\left[\left(ASN + offset_{ch}\right)\% n_{ch}\right] \quad (1)$$

where $f[\cdot]$ is a channel hopping sequence list (CHSL) which is a set of channels to be hopped over. *ASN* is the absolute slot number (ASN) which is the total number of timeslots that has elapsed since the start of the network. $offset_{ch}$ is the channel offset. n_{ch} is the number of channels in the CHSL.

All nodes operating in the TSCH network are globally time-synchronized through the enhanced beacon (EB) broadcasted periodically by coordinator. The EB includes ASN, CHSL, initial link information, etc. After the network configuration and formation is completed, nodes perform cell allocation for transmitting data packets to their parents according to the TSCH scheduling scheme. However, the TSCH scheduling scheme is not specified in the IEEE 802.15.4-2015 standard. IETF 6TiSCH working group defined 6TiSCH operational sublayer (6top) which provides management interfaces for cell scheduling between nodes [7]. It also defined 6top protocol (6P) which allows nodes to add/delete/relocate cells to their schedule through 6P transaction triggered by the scheduling function. The 6P transaction consists of either two or three steps (i.e., two-step 6P transaction and three-step 6P transaction), depending on which of the nodes transmitting or receiving 6P Request messages can select cells to be allocated.

Fig. 2. illustrates an example of two-step 6P transaction. Node A transmits a 6P ADD request message including the number of cells (i.e., NumCells) and the list of candidate cells (i.e., CellList) to Node B. Node B selects the number of available cells corresponding to NumCells from CellList by referring to its schedule and transmits 6P Response message

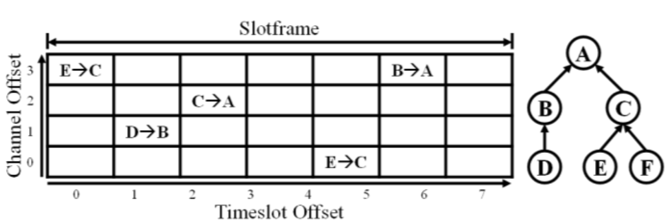

Fig. 1. TSCH slotframe structure and network topology.

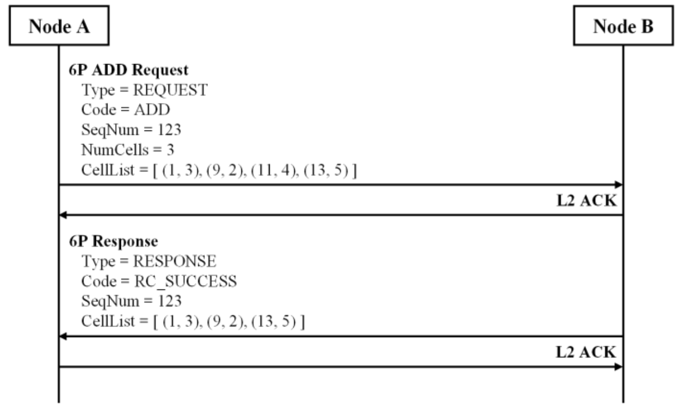

Fig. 2. Example of two-step 6P transaction.

including CellList to Node A. After the 6P transaction is completed, Nodes A and B allocate the selected cells to their schedules.

III. SYSTEM MODEL

Fig. 3. illustrates a system architecture of TSCH-based WPSN, which is considered a cluster-tree network topology consisting of HAPs and sensor nodes. In the network, a cluster is composed of one HAP and sensor nodes, where the HAP and the sensor node act as a cluster head and a cluster member, respectively. Only HAP can serve as the cluster head and be selected as a parent node of HAP and sensor node. The HAP supplies power to sensor nodes (i.e., cluster members) by using energy beamforming and transmits data received from sensor nodes to the neighboring HAP (i.e., parent) towards the root. It is equipped with a directional antenna for WPT and an omnidirectional antenna for data communication. The sensor node harvests energy from the HAP (i.e., cluster head) and transmits data to the HAP. It is battery-powered and is equipped with an omnidirectional antenna.

In TSCH-based WPSN, the amount of energy harvested by the sensor node per second can be affected by the transmission power of the HAP, the antenna gain of transmitter and receiver, and the distance between the HAP and the sensor node, calculated as follows:

$$P_r = P_t G_t G_r \left(\frac{\lambda}{4\pi}\right)^2 d^{-\alpha} \quad (2)$$

where P_r is the received power of the sensor node and P_t is the

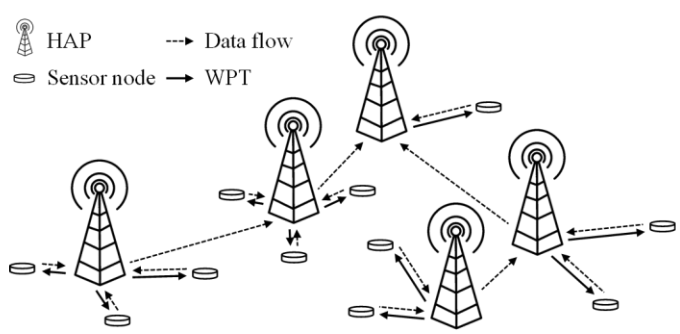

Fig. 3. System architecture of TSCH-based WPSN.

transmission power of the HAP. G_t and G_r are the antenna gain of the HAP and the sensor node, respectively. λ is the wavelength, d is the distance between the HAP and the sensor node, and α is the path loss exponent. Thus, the amount of energy harvested by the sensor node during a timeslot can be calculated as follows:

$$P_{Rx} = \eta P_r L_{timeslot} \tag{3}$$

where η is the energy harvesting efficiency factor and $L_{timeslot}$ is the length of timeslot.

In addition, the amount of energy consumed by the sensor node in each state (i.e., transmission (Tx), reception (Rx), idle, and sleep) during a timeslot (i.e., E_{Tx}, E_{Rx}, E_{Idle}, and E_{Sleep}) can be calculated as follows:

$$E_{Tx} = E_{sleep} L_{TsTxOffset} + E_{tx} L_{data} + E_{idle} L_{TsRxAckDelay} + E_{rx} L_{Ack} \tag{4}$$

$$E_{Rx} = E_{sleep} L_{TsRxOffset} + E_{rx} L_{data} + E_{idle} L_{TsTxAckDelay} + E_{tx} L_{Ack} \tag{5}$$

$$E_{Idle} = E_{idle} L_{timeslot} \tag{6}$$

$$E_{Sleep} = E_{sleep} L_{timeslot} \tag{7}$$

where E_{sleep}, E_{tx}, E_{idle}, and E_{rx} are the amount of energy consumed by the sensor node in sleep, Tx, idle, and Rx states during a timeslot, respectively. $L_{TsTxOffset}$ and $L_{TsRxAckDelay}$ are the time durations the sensor node waits to transmit the data packet and receive the acknowledgment (Ack), respectively. $L_{TsRxOffset}$ and $L_{TsTxAckDelay}$ are the time durations the sensor node waits to receive the data packet and transmit the Ack, respectively.

The sensor node calculates the number of cells required for energy harvesting (i.e., EH cells) based on the amount of energy harvested and consumed itself. After that, it performs cell allocation by transmitting a 6P ADD Request message including the number of cells required for data transmission (i.e., data cells) and EH cells, and then completes the 6P transaction.

IV. Simulation

A. Simulation Configuratoin

The experimental simulation was performed to investigate the impact of the slotframe length on the total amount of energy harvested by sensor nodes, aggregate throughput, and average end-to-end delay under the IEEE 802.15.4 TSCH network using MATLAB simulator. In the simulation, a cluster-tree network topology consisting of five HAPs and sensor nodes is considered. The number of sensor nodes varies from 4 to 40. Each HAP is randomly deployed within the coverage area of one of the neighboring HAPs. An equal number of sensor nodes are randomly deployed within a distance of 2 m from HAPs except the root HAP. The slotframe length was set to 50, 100, 150, and 200 timeslots. The number of data packets generated by each sensor node per second (i.e., traffic load) was set to 1 and 4. Table I shows the simulation parameters in detail.

TABLE I. Simulation Parameters

Parameter	Value	Parameter	Value
PHY/MAC	IEEE 802.15.4	P_t	100 mW
Number of sensor nodes	4–40	E_{Tx}	20.98 mA
Packet size	127 bytes	E_{Rx}	17.96 mA
Number of Data packets	1, 4	E_{Idle}	0.001 mA
Timeslot length	10 ms	E_{Sleep}	0.001 mA
Slotframe length	50, 100, 150, 200 timeslots	α	2.7
d	0–2 m	η	0.65

B. Simulation Results

Figs. 4(a) and (b) show the total amount of harvested energy when the traffic load is 1 and 4, respectively. In Fig. 4(a), when the number of sensor nodes is less than 32, the shorter the slotframe length, the higher the total amount of harvested energy. This is because a shorter slotframe enables the sensor nodes that have successfully allocated EH cells in the slotframe (i.e., successful nodes) to harvest energy more frequently. The total amount of harvested energy increases as the number of successful nodes increases. However, after a sensor node that fails to allocate EH cells in the slotframe (i.e., failed node) occurs, the total amount of harvested energy is maintained at a similar point regardless of the number of sensor nodes and the slotframe length. Therefore, in Fig 4(a), the total amount of harvested energy for slotframe lengths 50 and 100 is approximately equal when the number of sensor nodes is greater

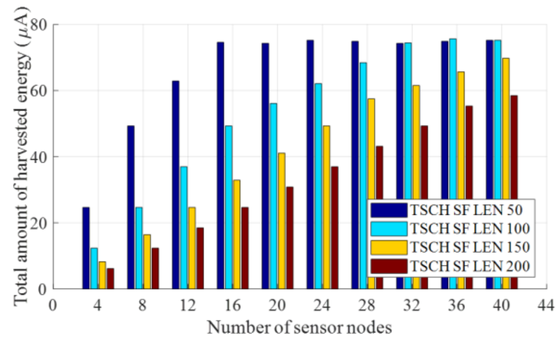

(a)

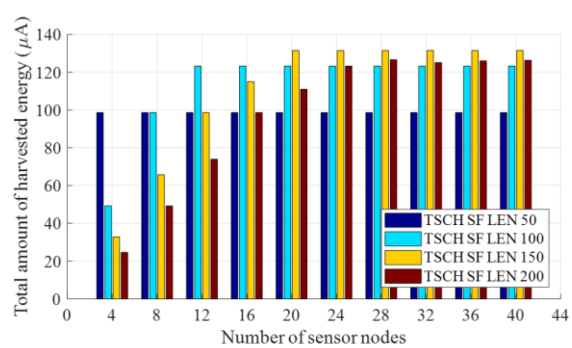

(b)

Fig. 4. Total amount of harvested energy: (a) traffic load of 1; (b) traffic load of 4.

than 28. In the case that the traffic load increases from 1 to 4, the number of EH cells allocated by sensor nodes increases. Therefore, the total amount of harvested energy in Fig. 4(b) is greater than that of Fig. 4(a). In this case, the total amount of harvested energy is saturated at a less number of sensor nodes compared to the other case. This is because the number of cells available for allocation in the slotframe further decreases whenever the number of sensor nodes increases.

Figs. 5(a) and (b) show the aggregate throughput when the traffic load is 1 and 4, respectively. In Fig. 5(a), as the number of sensor nodes increases, the aggregate throughput increases and then remains constant. This is because the number of data packets transmitted to the root HAP increases as the number of successful nodes increases. However, the number of cells allocated within the slotframe is limited due to the fixed slotframe length. Thus, if there are not enough available cells in the slotframe, the aggregate throughput does not increase. When the number of sensor nodes is less than 12, slotframes with lengths 50 and 100 achieve the highest aggregate throughput. This is because the slotframes are frequently repeated compared to other slotframes while sufficiently accommodating data packets within the network. However, when the number of sensor nodes is greater than 8, slotframes with length 100 or 150 achieve the highest aggregate throughput. This is because they allow more sensor nodes to successfully allocate data cells in the slotframe. This leads to an increase in the number of data packets arriving at the root HAP. Fig. 5(b) illustrates that the aggregate throughput is rapidly saturated than that of Fig. 5(a) in terms of the change in traffic load. This is because, when the traffic load increases from 1 to 4, even if only a small number of sensor nodes perform cell allocation, the number of allocated data cells reaches the number of data cells that the slotframe can accommodate.

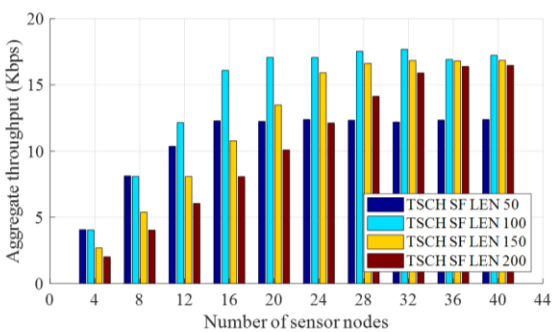

(a)

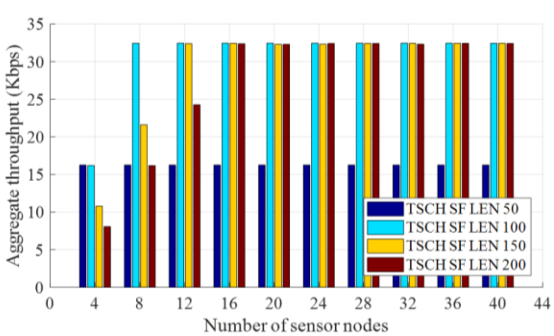

(b)

Fig. 5. Aggregate throughput: (a) traffic load of 1; (b) traffic load of 4.

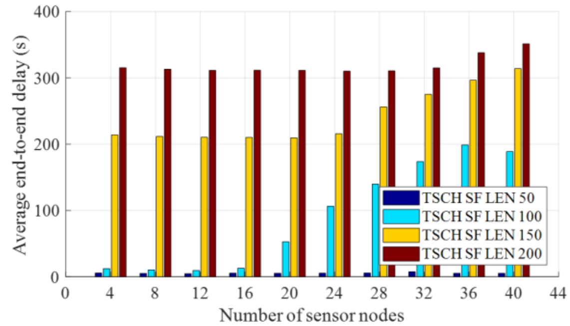

(a)

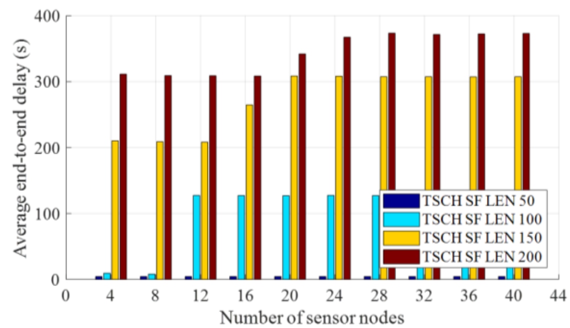

(b)

Fig. 6. Average end-to-end delay: (a) traffic load of 1; (b) traffic load of 4.

Figs. 6(a) and (b) show the average end-to-end delay when the traffic load is 1 and 4, respectively. Overall, the shorter the slotframe length, the shorter the average end-to-end delay, regardless of the traffic load. This is because the period of data transmission of the sensor node is proportional to the slotframe length. In TSCH-based WPSN, the average end-to-end delay tends to remain constant and then increase as the number of sensor nodes increases. Until the number of sensor nodes reaches a certain number, the average end-to-end delay is maintained constant as a result of transmission delay due to cell allocation of HAPs and sensor nodes. However, when the number of sensor nodes exceeds a certain number, the average end-to-end delay increases because HAPs receive more data packets than the number of packets that can be transmitted in one slotframe. In this respect, the average end-to-end delay is shorter when the traffic load is 1 compared to 4.

V. Conclusion

This paper presents the impact of slotframe length on the performance of TSCH-based WPSN. The simulation was performed under environments in which the network size and traffic load varies in order to analyze the network performance according to the change of slotframe length. The simulation results showed that the slotframe length that maximizes the total amount of harvested energy and aggregate throughput depends on the number of sensor nodes and data packets transmitted by the sensor nodes in the network. In addition, the long slotframe length causes the long average end-to-end delay. Consequently, in order to achieve better TSCH-based WPSN performance, the slotframe length needs to be set as short as possible considering the network size and traffic load.

ACKNOWLEDGMENT

This research was supported by Basic Science Research Program through the National Research Foundation of Korea (NRF) funded by the Ministry of Education (NRF-2020R1I1A3052733). This work was supported by the NRF grant funded by the Korea government (MSIT) (NRF-2021R1C1C2095696).

REFERENCES

[1] M. A. Jamshed, K. Ali, Q. H. Abbasi, M. A. Imran, and M. Ur-Rehman, "Challenges, applications, and future of wireless sensors in Internet of Things: A review," IEEE Sensors J., vol. 22, no. 6, pp. 5482–5494, Mar. 2022.

[2] M. A. Albreem, A. M. Sheikh, M. H. Alsharif, M. Jusoh, and M. N. M. Yasin, "Green Internet of Things (GIoT): Applications, Practices, Awareness, and Challenges," IEEE Access, vol. 9, pp. 38833–38858, Feb. 2021.

[3] A. H. Ngu, M. Gutierrez, V. Metsis, S. Nepal, and Q. Z. Sheng, "IoT middleware: A survey on issues and enabling technologies," IEEE Internet Things J., vol. 4, no. 1, pp. 1–20, Feb. 2017.

[4] S. M. A. Huda, M. Y. Arafat, and S. Moh, "Wireless Power Transfer in Wirelessly Powered Sensor Networks: A Review of Recent Progress," Sensors, vol. 22, no. 8, p. 2952, Apr. 2022.

[5] M. A. Ullah, R. Keshavarz, M. Abolhasan, J. Lipman, K. P. Esselle, and N. Shariati, "A review on antenna technologies for ambient RF energy harvesting and wireless power transfer: Designs, challenges and applications," IEEE Access, vol. 10, pp. 17231–17267, Feb. 2022.

[6] IEEE Standard for Low-Rate Wireless Networks, IEEE Standard 802.15.4-2015, Apr. 2016.

[7] Q. Wang, X. Vilajosana, and T. Watteyne, 6top Protocol (6P), Internet Engineering Task Force Std. document RFC8480, Aug. 2018.